Grazing Incidence Diffraction and Brewster-Angle Microscope Studies of Mixtures of Hexadecanoic Acid and Methyl Hexadecanoate: The Unexpected Appearance of a Phase with Nearest-Neighbor Tilt

Ellis Teer and Charles M. Knobler*

Department of Chemistry and Biochemistry, University of California, Los Angeles, California 90095-1569

Stefan Siegel, Dieter Vollhardt, and Gerald Brezesinski*

Max Planck Institute of Colloids and Surfaces, D-14476 Golm/Potsdam, Germany

Received: June 21, 2000; In Final Form: August 25, 2000

To examine the relative stability of monolayer phases with nearest-neighbor (NN) and next-nearest-neighbor (NNN) tilt directions, we have performed grazing incidence X-ray diffraction and Brewster-angle microscopy studies on mixtures of hexadecanoic acid with methyl *n*-hexadecanoate. We have determined how the boundary between the L_2 (NN) and Ov (NNN) phases change with composition. Beyond a mole fraction of ester $x = 0.70$, the boundary moves sharply toward lower temperature with increasing concentration of the ester, and eventually the only tilted mesophase remaining has NN tilt. This is in contrast to many other esters that have been studied for which there is only a NNN mesophase. It is argued that the stability of the NN phase is the result of disorder in the chain ends of the amphiphile.

Introduction

The complexities of the Langmuir monolayer phase diagrams of simple amphiphiles such as saturated fatty acids and their esters were first described by early workers such as Stenhagen[1] and Lundquist[2], who located phase boundaries from precise measurements of the surface pressure as a function of the area. They were able to assign structures to the phases by correlating their properties with those of three-dimensional polymorphs whose structures had been determined from diffraction measurements.

With the advent of synchrotron grazing-incidence X-ray diffraction (GIXD) experiments, structures of Langmuir monolayers could be determined directly,[3] and with the development of imaging methods such as Brewster-angle microscopy,[4,5] it became possible to locate phase boundaries visually.[6] The application of these methods to the study of monolayers of acids has shown that the phase diagrams determined from thermodynamic measurements were essentially correct but incomplete. There is a generic diagram (Figure 1) that applies to all of the acid homologues studied and it is simply shifted in temperature in proportion to the chain length. Of the seven condensed phases shown in the diagram, only one, the Ov phase, was not recognized in the early studies. In the CS, S, and LS phases the hydrocarbon-chain backbones are perpendicular to the interface; the chains are tilted in the L_2'', L_2', L_2 and Ov phases. Only the CS and L_2'' phases are crystalline; the other condensed phases are mesophases. The tilted phases can be distinguished in part by the direction of the tilt azimuth: in the L_2 and L_2'' phases the tilt is toward nearest neighbors (NN) while it is toward next-nearest neighbors (NNN) in the L_2' and Ov phases.[7] The other two phases shown in Figure 1 are the liquid expanded phase (LE) and the gaseous phase (G), both of which are isotropic.

The situation is less clear with the esters. Lundquist[2] carried out isotherm studies of the homologous series ethyl *n*-hexadecanoate to ethyl *n*-heneicosanoate and found a generic diagram

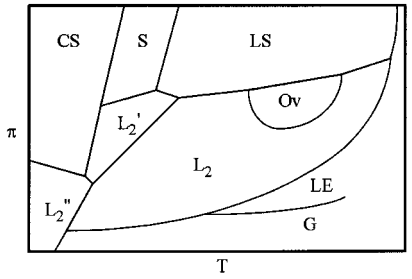

Figure 1. Schematic surface pressure−temperature monolayer phase diagram for a saturated fatty acid. The liquid expanded (LE) and gaseous (G) phases are isotropic. The other more condensed phases are not.

that differed from that of the acids in that there was only a single tilted phase at high temperature, L_2'. In contrast, Bibo et al.[8] reported that in ethyl *n*-eicosanoate the tilt was toward nearest neighbors in the corresponding region of the phase diagram, i.e., that the phase was L_2. The phase diagram for methyl *n*-eicosanoate determined from an extensive GIXD study[9] agrees with that of Lundquist in that the tilt direction in the high-temperature tilted phase is NNN. Teer et al.[10] reached a similar conclusion. They employed BAM to trace the motion of the phase boundaries as fatty acids were mixed with their esters, which made it possible to identify the ester phases. The phase diagrams for methyl and ethyl *n*-heneicosanoate and methyl, ethyl, and propyl *n*-octadecanoate were all found to be in accord with that for methyl *n*-eicosanoate determined by Foster et al.[9] Recent GIXD measurements on a mixture of octadecanoic acid and methyl *n*-octadecanoate[11] are also consistent with the BAM measurements and those on the pure ester.

The mixture studies showed that the NNN phase in the esters could be thought of as arising from a merger of the L_2' and Ov phases. With increasing concentration of the ester, the L_2'/L_2 phase boundary moves toward higher temperature and lower pressure while the Ov/L_2 boundary moves toward lower

10.1021/jp002254c CCC: $19.00
Published on Web 10/07/2000

temperature and lower pressure. At still higher concentrations the L_2' and Ov phases merge and the boundary with the L_2 phase is driven to zero pressure, leaving what appears from BAM measurements to be a single NNN phase. GIXD studies show that the merged phase has the L_2' structure at low temperature and that of the Ov phase at high temperature. Foster et al.[9] argued that there are two distinct NNN phases. Studies on an acid−ester mixture[11] show a narrow region of temperature in which there is a continuous transition between the two kinds of structure.

The picture that seemed to emerge from the studies on acids, alcohols, esters, and their mixtures[10] was that there are two general types of phase diagrams. In the one that applies to acids and to acetate esters of *n*-alkanols, there are three distinct noncrystalline tilted mesophases: L_2' (NNN), Ov(NNN), and L_2 (NN). In the other diagram, which applies to esters of saturated fatty acids and to saturated alcohols,[11,12] there is no NN phase and the L_2' and Ov phases are merged. The controlling factor appeared to be the maximum tilt angle, which is related to the headgroup size. If the headgroup is small, the maximum tilt angle is small and there is a single NNN phase. The tilt angle increases with headgroup size and large tilt angles are associated with the existence of an NN phase, with no obvious dependence on chain length.

In a recent paper, however, Weidemann et al.[13] described GIXD measurements on several esters at a single temperature just below the transition to the liquid expanded phase. In accord with the earlier studies of esters, for ethyl *n*-hexadecanoate they found a NNN phase that underwent a transition to an untilted phase at high pressure. In the case of methyl *n*-hexadecanoate, however, only a NN phase was observed, a result that was not consistent with our expectations about the phase diagrams of esters and the relation between headgroup size and the stability of tilted phases. We have therefore examined the phase diagram of methyl *n*-hexadecanoate in more detail by both GIXD and BAM investigations of the evolution of phase boundaries in acid−ester mixtures.

Experimental Section

The BAM measurements were carried out at UCLA using the apparatus previously described in detail.[14] Hexadecanoic acid (99+%) and methyl *n*-hexadecanoate were obtained from Nu-Chek Prep and used without further purification. Acid−ester mixtures in chloroform (p.a. Merck) were spread onto pure water (Millipore Milli-Q, 18 MΩ) in a homemade Teflon trough. Pressures were measured with a filter-paper Wilhelmy plate. The phase boundaries were detected as abrupt changes in the optical texture when the surface pressure was changed at constant temperature and were observed both on compression and expansion. They could generally be determined with a precision of 0.2 mN m^{-1}.

For the X-ray experiments, hexadecanoic acid and methyl *n*-hexadecanoate were obtained from Sigma (Deisenhofen) and used without further purification. The monolayers were spread from a 1 mM chloroform solution onto a subphase consisting of ultrapure water. The experiments were performed using the liquid-surface diffractometer on the undulator beamline BW1 at HASYLAB, DESY, Hamburg, Germany. A monochromatic synchrotron beam strikes the air/water interface at grazing incidence angle $\alpha_i = 0.85\alpha_c$, where $\alpha_c \sim 0.14°$ is the critical angle for total reflection. The diffracted intensity is detected by a linear position-sensitive detector (PSD) (OED-100-M, Braun, Garching, Germany) as a function of the vertical scattering angle α_f. A Soller collimator is located in front of the PSD and provides the resolution for the horizontal scattering angle $2\theta_{xy}$. The scattering of X-rays is elastic, and therefore the wave vectors $\boldsymbol{k}_i$ and $\boldsymbol{k}_f$ of the incident and diffracted photons have the same absolute value. The horizontal (in-plane) component of the scattering vector $\mathbf{Q} = \boldsymbol{k}_f - \boldsymbol{k}_i$ is given by $Q_{xy} \approx (4\pi/\lambda)\sin(\theta_{xy})$ and the vertical (out-of-plane) component is given by $Q_z \approx (2\pi/\lambda)\sin(\alpha_f)$, where λ is the X-ray wavelength.[15−17] The diffracted intensities were corrected for polarization, effective area, and Lorentz factor. Model peaks taken to be Lorentzian in the in-plane direction and Gaussian in the out-of-plane direction were fitted to the corrected intensities.

Results

GIXD. Most of the diffraction studies were carried out at 20 °C but a few measurements were performed at 4 °C. In addition to the pure acid and ester, we studied eight mixtures at different surface pressures. In the experiments described below, the structures are either centered-rectangular or hexagonal. In the case of a rectangular structure with tilted molecules, only two diffraction peaks are observed in the powder pattern. Figure 2 shows contour plots of the corrected intensities as a function of the in-plane scattering vector component Q_{xy} and the out-of-plane scattering vector component Q_z for the pure compounds and two mixtures. An intensity distribution with the nondegenerate peak located at $Q_z = 0$ and the degenerate one at $Q_z > 0$ indicates a tilt in a symmetry direction toward nearest neighbors. If both peaks of the centered-rectangular lattice are located at $Q_z > 0$ (with $Q_z^n = 2Q_z^d$, where Q_z^n is the position of the maximum of the nondegenerate peak and Q_z^d that of the 2-fold degenerate one) the tilt direction is toward next-nearest neighbors.[3]

Some of the experiments have been analyzed quantitatively. The lattice parameters can be obtained from the peak positions. The lattice spacing is given by $d(hk) = 2\pi/Q_{xy}^{hk}$, where (h,k) denotes the order of the reflection. The tilt angle with respect to the surface normal can be calculated from ref 18.

$$\tan t = Q_z^d/\sqrt{(Q_{xy}^n)^2 - (Q_{xy}^d)^2}, \quad \text{if } Q_z^n = 0$$

$$\tan t = Q_z^n/Q_{xy}^n \quad \text{if } Q_z^n > 0$$

The cross-sectional area of the chains is given by $A_0 = A_{xy}\cos(t)$, where A_{xy} is the area per molecule in the water plane. These results are shown in Table 1, which gives the unit cell parameters, the in-plane lattice area, the chain tilt angle and tilt direction, the distortion in a plane perpendicular to the chains, and the lattice distortion.

The measurements for the pure compounds are in complete accord with the previous study.[13] In the pure acid there is a NN phase at low pressure and a transition to a NNN phase above 16.5 mN m^{-1}; these correspond to the L_2 and Ov phases. Only a NN phase is observed in the pure ester. The untilted phase appears at 10.0 mN m^{-1}. From the isotherms we deduce a linear dependence of the molecular area on the surface pressure. This dependence can be described as $A_{xy} = K_1 - K_2\pi$. Assuming that the cross-sectional area A_0 does not depend on the surface pressure (see Table 1), $1/\cos(t)$ must be a linear function of the surface pressure. This relation can be used to determine the pressure of the transition to the untilted phase as shown in Figure 3 for two mixtures, $x = 0.67$ and $x = 0.75$. The extrapolated pressures, 11.1 and 10.2 mNm^{-1}, respectively, correspond very well with the kinks in the isotherms.

There is no evidence in the diffraction studies of the mixtures of two distinct sets of peaks, one belonging to the acid and the

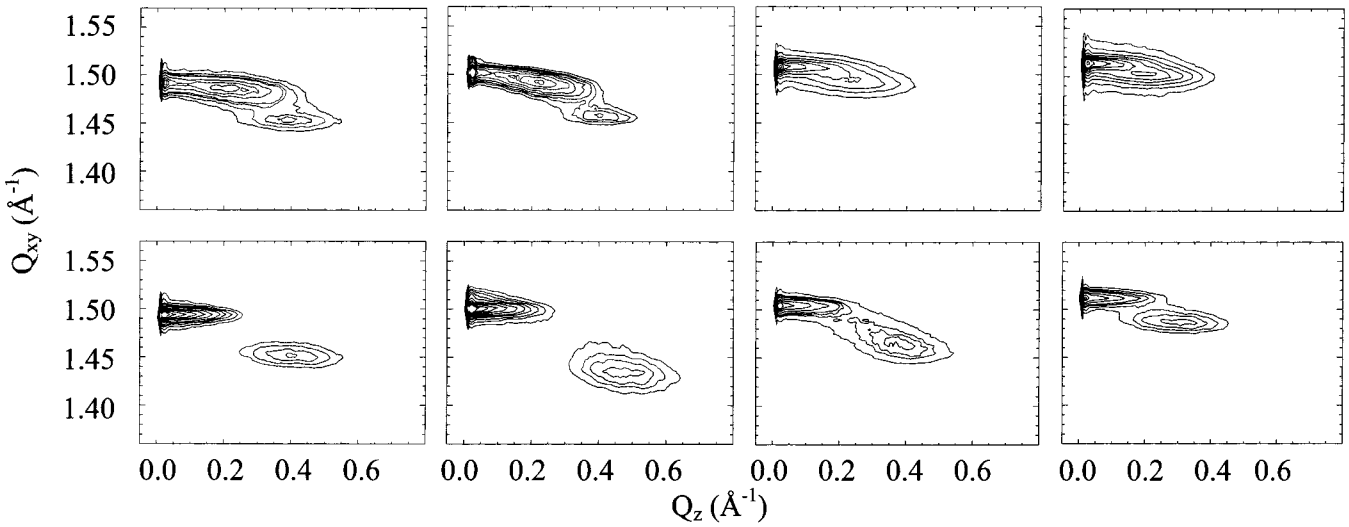

Figure 2. Contour plots of the corrected X-ray intensities for hexadecanoic acid, methyl *n*-hexadecanoate, and two mixtures. The intensities of the in-plane component Q_{xy} of the scattering vector **Q** are plotted versus those of *the* out-of-plane component Q_z. Hexadecanoic acid (left) at 18.4 mN/m (top) and 16.5 mN/m (bottom). Mixtures, $x = 0.71$ (second from left) at 5.5 mN/m (top) and 1.8 mN/m (bottom); $x = 0.75$ (second from right) at 8.0 mN/m (top) and 4.5 mN/m (bottom); methyl *n*-hexadecanoate (right) at 7.1 mN/m (top) and 5.0 mN/m (bottom) at 20 °C. *x* is the mole fraction of the ester.

other to the ester. The mixtures are therefore homogeneous and the path between the acid and the ester can be followed by examining the variation of the phase boundaries with composition. As in previous studies of mixtures,[10] the pressure of the NN/NNN transition is markedly lower in the mixture with a mole fraction of ester $x = 0.25$ than it is in the pure acid. It decreases further with increasing concentration of ester, and reaches a value between 1.8 and 3.7 mN m^{-1} by $x = 0.71$. But at $x = 0.75$, the NNN phase is absent; the NN phase is present even at 10 mN m^{-1}, just short of the extrapolated value of the pressure at the transition to the untilted phase, 10.2 mN m^{-1}. There is no evidence of a NNN phase at compositions ≥ 0.75. Thus, from the GIXD measurements it appears that the NN/NNN transition pressure drops to a minimum and then rises abruptly with just a 0.04 increase in the mole fraction of the ester.

Additional diffraction measurements were performed at 4 °C for the pure ester and for two mixtures in the concentration region where the NN/NNN transition pressure appears to rise markedly. Again, the pure ester exhibits only the NN-tilted phase as does the mixture with $x = 0.80$. However, in the mixture with $x = 0.75$, for which there is only the NN phase at 20 °C, there is now a NNN-tilted phase from 3 to 9.5 mN m^{-1}. The extrapolated transition to the untilted phase is now 11.3 mN m^{-1}. Thus, the NN/NNN transition line moves to slightly larger mole fraction of the ester with decreasing temperature. The decrease in temperature also leads to a decrease in the cross-sectional area, as expected. For these mixtures A_0 is 19.5 Å^2 compared to 19.9 Å^2 at 20 °C. This smaller area indicates a closer packing of the molecules and a reduced mobility.

More information about the packing can be obtained from the values of the distortion (see Table 1). The distortion of the unit cell, ξ, is defined as $\xi = (l_1^2 - l_2^2)/(l_1^2 + l_2^2)$, where l_1 and l_2 are the major and minor axes, respectively, of the ellipse passing through all six nearest neighbors of a molecule. The signed distortion, d, is defined as $d = \xi \cos 2(\omega - \beta)$, where ω and β are the azimuths of the lattice distortion and of the tilt, respectively. A linear dependence of d on $\sin^2(t)$ has been deduced from Landau theory[18] and, as shown in Figure 4, our data are consistent with such a relationship. In the absence of backbone order, d_0, the intercept of the plot at $\sin^2(t) = 0$, should be zero. The lines in Figure 5 extrapolate to d_0 values between 0.003 and −0.002, which demonstrates that there is negligible backbone order. The molecules are in a rotator phase both at 20 and 4 °C.

BAM. The evolution of the phase diagram becomes clearer from the BAM studies. Measurements were made at temperatures between 0 and 30 °C for the pure acid and many compositions of the mixture; a sampling of the diagrams is shown in Figure 5. One expects that the phase diagram of the acid will shift downward in temperature by an average of about 6 K per methylene group[19] so that the maximum temperature of the L_2'/L_2 boundary, which lies at 28 °C in docosanoic acid,[6] would be inaccessible in measurements of hexadecanoic acid. This indeed is the case and only the L_2/Ov boundary and the transitions to the untilted phases and to the LE phase can be seen.

At first, as seen in other acid−ester mixtures, the L_2/Ov boundary moves downward in pressure with the addition of the ester. Note, however, that the boundary does not extend to the LE phase; there is a small region at high temperature in which the L_2 phase extends to the transition to the untilted phase. At ester mole fractions above 0.70, the high-temperature side of the L_2/Ov phase boundary begins to move toward lower temperature and as the concentration of ester is increased the extent of the L_2 phase grows at the expense of the Ov phase. As a result, in this ester the tilt direction in the high-temperature phase is toward nearest neighbors rather than toward next-nearest neighbors as observed for its longer-chain homologues. What appeared from the GIXD measurements to be a rapid shift of the L_2/Ov boundary to higher pressure is shown by the BAM experiments to be a shift of the boundary with temperature.

The GIXD and BAM data are brought together in the surface pressure−composition phase diagram shown in Figure 6, which shows data obtained at 20 °C. The points distinguish the different phase types determined by GIXD and the phase boundaries determined by BAM. Included in the plot are diffraction measurements that are not presented in Table 1 in which only a qualitative determination of the phase type (NN or NNN) was made. The BAM and GIXD data for the tilted−

TABLE 1: Data Derived from GIXD Measurements of Hexadecanoic Acid, Methyl *n*-Hexadecanoate, and Their Mixtures[a]

π (mN/m)	a_r (Å)	b_r (Å)	A_{xy} (Å^2)	t (deg)	tilt direction	A_0 (Å^2)	d
			$T = 20$ °C				
			$x = 0.00$				
14.5	5.105	8.428	21.5	19.9	NN	20.2	0.047 88
16.5	5.046	8.410	21.2	17.7	NN	20.2	0.038 37
18.4	4.843	8.648	20.9	15.9	NNN	20.1	0.030 60
			$x = 0.25$				
9.2	5.117	8.417	21.5	20.7	NN	20.1	0.051 61
11.0	4.847	8.744	21.2	17.1	NNN	20.2	0.040 68
12.9	4.839	8.644	20.9	15.7	NNN	20.1	0.030 58
			$x = 0.50$				
3.0	5.156	8.440	21.8	22.1	NN	20.2	0.056 53
6.0	4.844	8.787	21.3	18.6	NNN	20.2	0.046 17
17.0	4.798	8.310	19.9	0		19.9	0
			$x = 0.67$				
1.8	5.129	8.407	21.6	21.4	NN	20.1	0.055 34
3.7	4.867	8.781	21.4	19.7	NNN	20.1	0.040 85
6.4	4.813	8.578	20.6	15.3	NNN	19.9	0.028 60
7.8	4.809	8.502	20.4	13.2	NNN	19.9	0.020 48
8.6	4.804	8.461	20.3	11.4	NNN	19.9	0.016 88
10.1	4.805	8.410	20.2	7.5	NNN	20.0	0.010 64
			$x = 0.71$				
1.8	5.132	8.372	21.5	21.2	NN	20.0	0.059 87
3.7	4.807	8.684	20.9	18.2	NNN	19.8	0.042 16
5.5	4.836	8.636	20.9	16.2	NNN	20.0	0.030 56
			$x = 0.75$				
2.5	5.035	8.355	21.0	18.4	NN	20.0	0.042 77
4.5	4.997	8.356	20.9	16.6	NN	20.0	0.035 33
5.0	4.970	8.355	20.8	14.4	NN	20.1	0.029 80
7.5	4.872	8.333	20.3	10.7	NN	19.9	0.012 48
8.0	4.876	8.332	20.3	10.9	NN	19.9	0.013 37
10.0	4.789	8.295	19.9	1	NN	19.9	0
15.0	4.783	8.284	19.8	0		19.8	0
			$x = 0.80$				
3.0	5.005	8.322	20.8	17.6	NN	19.8	0.040 74
5.5	4.899	8.306	20.3	13.0	NN	19.8	0.021 43
8.0	4.825	8.306	20.0	9.4	NN	19.8	0.006 19
12.0	4.779	8.278	19.8	0		19.8	0
			$x = 0.90$				
3.0	4.993	8.333	20.8	17.4	NN	19.9	0.037 08
6.9	4.857	8.318	20.2	10.5	NN	19.9	0.011 55
9.1	4.789	8.295	19.9	0		19.9	0
			$x = 0.95$				
1.0	5.029	8.339	21.0	18.8	NN	19.8	0.043 62
5.0	4.918	8.321	20.5	12.8	NN	20.0	0.023 29
7.0	4.825	8.350	20.1	9.5	NN	19.9	0.000 89
9.1	4.786	8.290	19.8	0		19.8	0
			$x = 1.00$				
1.1	5.035	8.333	21.0	18.4	NN	19.9	0.045 45
5.0	4.907	8.312	20.4	12.9	NN	19.9	0.022 35
7.1	4.847	8.305	20.1	9.8	NN	19.8	0.010 64
10.0	4.787	8.291	19.8	0		19.8	0
			$T = 4$ °C				
			$x = 0.75$				
3.0	4.785	8.690	20.8	17.6	NNN	19.8	0.0476
6.0	4.770	8.485	20.2	14.4	NNN	19.6	0.026 558
9.5	4.783	8.284	19.8	8.3	NNN	19.6	0
15.0	4.748	8.224	19.5	0		19.5	0
			$x = 0.80$				
2.5	5.009	8.240	20.6	19.2	NN	19.5	0.051 42
6.0	4.891	8.219	20.1	14.3	NN	19.5	0.030 20
9.5	4.778	8.219	19.6	9.5	NN	19.4	0.007 01
11.0	4.745	8.219	19.5	1.8	NN	19.5	0
14.0	4.739	8.208	19.4	0		19.4	0
			$x = 1.00$				
2.0	5.044	8.208	20.7	19.6	NN	19.5	0.062 40
5.0	4.924	8.208	20.2	15.1	NN	19.5	0.038 34
8.0	4.801	8.213	19.7	9.5	NN	19.4	0.012 29
12.0	4.742	8.213	19.5	0		19.5	0

[a] x is the mole fraction of ester, a_r and b_r are the lattice parameters of the centered rectangular unit cell, A_{xy} is the in-plane lattice area, t is the tilt angle, A_0 is the cross-sectional area perpendicular to the chains, and d is the signed lattice distortion. The measurements were performed at 20 and 4 °C.

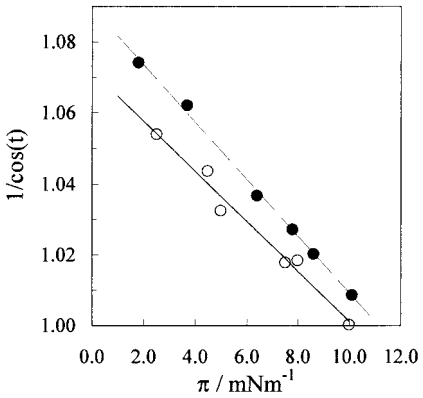

Figure 3. Plots of 1/cos(t) versus surface pressure for two mixtures: (●) $x = 0.67$; (○) $x = 0.75$. The extrapolation to zero tilt gives the pressure at the transition to the untilted phase.

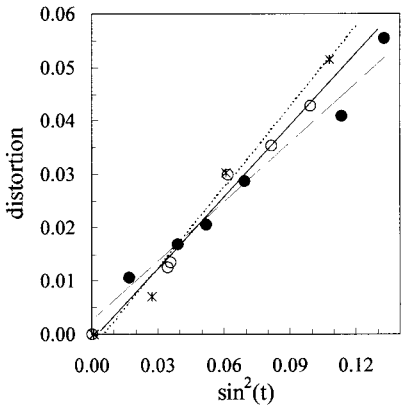

Figure 4. Plot of the signed distortion versus $\sin^2(t)$. Three different mixtures at different temperatures are shown: (○) $x = 0.75$ at 20 °C, (●) $x = 0.67$ at 20 °C and (∗) $x = 0.80$ at 4 °C.

untilted transition agree well but there are larger differences in the location of the boundary between the tilted phases. These can be attributed to small systematic differences between the compositions of the mixtures prepared in the two laboratories and the very high sensitivity of the boundary to composition.

In summary, both the GIXD and BAM measurements demonstrate that in contrast to the other esters that had earlier been examined, in monolayers of methyl *n*-hexadecanoate the tilt in the high-temperature phase is toward nearest neighbors. The dilution studies show that the L_2 phase is stable at high temperatures and that the NNN Ov phase is displaced toward lower temperature with increasing concentration of ester.

Discussion

In retrospect, the enhanced stability of the L_2 phase with respect to the Ov phase with decreasing chain length should have been anticipated. In the BAM studies by Overbeck and Möbius in which the Ov phase was discovered in acids,[20] it was shown that the extent of the Ov region of the phase diagram decreased as the chain length was decreased from 20 to 16. These results show that the stability of the Ov phase decreases with decreasing chain length. Moreover, in smectic liquid crystals, NN phases, e.g., the hexatic F phase, always occur at higher temperature than their NNN equivalent, e.g., the I phase.[21] Thus, the analogies between smectic liquid crystalline phases and monolayer phases, which were first recognized by Peterson,[22] are seen now to be even stronger.

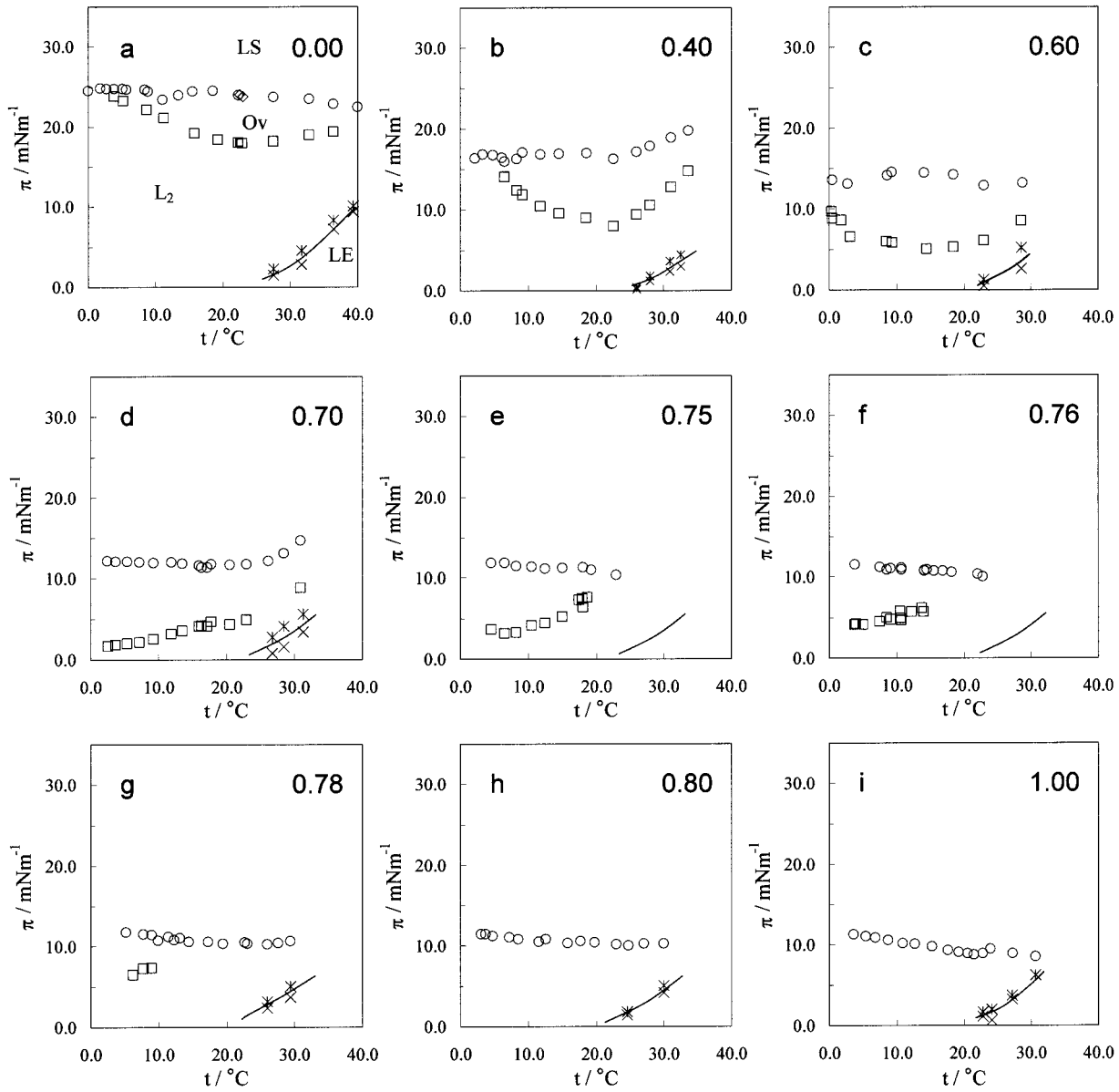

Figure 5. Surface pressure−temperature phase diagrams for hexadecanoic acid, methyl *n*-hexadecanoate, and their mixtures determined from BAM measurements. The mole fractions of ester are specified in each figure. The transition to the LE phase was observed in all cases but the data points were not recorded for mixtures e and f; lines in those figures give the approximate location of the transition. Hysteresis at the transition to the LE phase accounts for differences between points measured at the same temperature. Diagrams at other compositions are not shown because there was a smooth evolution of phase boundaries between the compositions presented here.

In the Landau theory of monolayer phases developed by Kaganer and co-workers,[3] the location of the L_2/Ov boundary is determined by the free energy

$$\Phi = A\eta^2 + B\eta^4 - Dh\eta^6 \cos 6(\beta - \gamma) + Eh^2\eta^{12} \cos 12(\beta - \gamma)$$

in which the first two terms involve the tilt order parameter $\eta = \sin t$, where t is the chain tilt angle, and the second two terms arise from the coupling between η and the hexatic order parameter h. The tilt direction of a phase is specified by the difference in the bond and tilt azimuths, $\beta - \gamma$. When $\beta - \gamma = 0$, the tilt direction is toward nearest neighbors and it is toward next-nearest neighbors when $\beta - \gamma = \pi/6$. The NN/NNN transition occurs on the line $D(\eta,T) = 0$. Although it was evident from the shape of the L_2/Ov boundary in the acids that this line had to go through a minimum in pressure, no physical reason for this behavior was given. It now seems likely that the high-temperature stability of the NN phase is associated with disorder in the chain ends. Since the interplanar spacing in a NN phase is greater than that in a NNN phase, this entropic contribution to the free energy will be higher in the L_2 phase than in the Ov phase. We should also expect chain-end disorder to play a larger role in shorter chains than in longer ones, so that the high-temperature region of the L_2 phase would be more extensive in the shorter-chain amphiphiles.

It is evident, however, that the relative stability of the tilted phases does not depend only on the chain length: the phase diagrams of the esters and alcohols differ from those of the corresponding acids and acetates. This effect of the headgroup, however, is more subtle than previously recognized. The GIXD measurements by Weidemann et al.[13] on *ethyl n*-hexadecanoate show that its phase diagram differs from that of *methyl n*-hexadecanoate. Its high-temperature tilted phase is NNN, i.e., its diagram is apparently similar to that of the longer-chain esters. Although there was no evidence of a NN phase at high

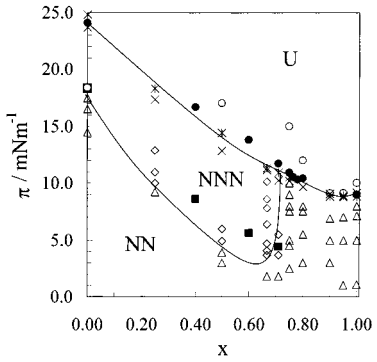

Figure 6. Surface pressure−composition phase diagram for the system hexadecanoic acid−methyl *n*-hexadecanoate. The points identify the phases determined by GIXD (△, NN phase, ◇, NNN phase, ○, untilted phase), the locations of the phase boundaries determined by BAM (■, NN/NNN transition, ●, tilted/untilted transition) and the tilted-untilted transition determined from the isotherms (×) and from plots of $1/\cos(t)$ against π (∗).

temperature in the other esters that have been studied, it may be possible that such a region does exist close to the transition to the LE phase and that it has been overlooked. More detailed studies at high temperature would show if this were the case. Finally, we note that monolayer phase diagrams that are intermediate between those of esters and acids have been observed for pure substances,[23] evidence again that the mixtures smoothly interpolate between the different phase types.

Acknowledgment. This work was supported by the U.S. National Science Foundation and the Deutsche Forschungsgemeinschaft. It arose out of discussions during a visit to the MPI by C.M.K. that was sponsored by the Alexander von Humboldt Foundation. We thank HASYLAB at DESY for beam time and support.

References and Notes

(1) Stenhagen, E. In *Determination of Organic Structures by Physical Methods;* Braude, E. A., Nachod, F. C., Eds.; Academic Press: New York, 1955.

(2) Lundquist, M. *Chem. Scr.* **1971**, *1*, 197.

(3) For a review see Kaganer, V.; Möhwald, H.; Dutta, P. *Rev. Mod. Phys.* **1999,** *71*, 779.

(4) Hönig, D.; Möbius, D. *J. Phys. Chem.* **1991**, *95*, 4590.

(5) Hénon, S.; Meunier, J. *Rev. Sci. Instr.* **1991**, *62*, 936.

(6) Rivière, S.; Hénon, S.; Meunier, J.; Schwartz, D. K.; Tsao, M.-W.; Knobler, C. M. *J. Phys. Chem.* **1994**, *101*, 10045.

(7) An additional tilted phase, in which the tilt is in a direction intermediate between NN and NNN, has also been observed in eicosanoic acid by GIXD (Durbin, M. K.; Malik, A.; Richter, A. G.; Ghaskadvi, R.; Gog, T.; Dutta, P. *J. Chem. Phys.* **1997**, *106*, 8216) and with BAM (Lautz, C.; Fischer, T. M. *Euro. Phys. J. B* **1999**, *7*, 263).

(8) Bibo, A. M.; Knobler, C. M.; Peterson, I. R. *J. Phys. Chem.* **1991**, *95*, 5591.

(9) Foster, W. J.; Shih, M. C.; Pershan, P. S. *J. Chem. Phys.* **1996**, *105*, 3307.

(10) Teer, E.; Knobler, C. M.; Wurlitzer, S.; Lautz, C.; Kildea, J.; Fischer, T. M. *J. Chem. Phys.* **1997**, *106*, 1913.

(11) Teer, E.; Knobler, C. M.; Braslau, A.; Daillant, J.; Blot, C.; Luzet, D.; Goldmann, M.; Fontiane, P. *J. Chem. Phys.* **2000**, *113*, 2846.

(12) Fischer, B.; Teer, E.; Knobler, C. M. *J. Chem. Phys.* **1995**, *103*, 2365.

(13) Weidemann, G.; Brezesinski, G.; Vollhardt, D.; Bringezu, F.; de Meijere, K.; Möhwald, H. *J. Phys. Chem.* **1998**, *102*, 148.

(14) Fisher, B.; Tsao, M.-W.; Ruiz-Garcia, J.; Fischer, T. M.; Schwartz, D. K..; Knobler, C. M. *J. Phys. Chem.* **1994**, *98*, 7430.

(15) Als-Nielsen, J.; Jaquemain, D.; Kjaer, K.; Lahav, M.; Leveiller, F.; Leiserowitz, L. *Phys. Rep.* **1994**, *246*, 251.

(16) Kjaer, K. *Physica B* **1994**, *198*, 100.

(17) Rietz, R.; Rettig, W.; Brezesinski, G.; Möhwald, H.; Bouwman, W. G.; Kjaer, K. *Thin Solid Films* **1996**, *284/285*, 211.

(18) Kaganer, V. M.; Peterson, I. R.; Kenn, R. M.; Shih, M. C.; Durbin, M.; Dutta, P. *J. Chem. Phys.* **1995**, *102*, 9412.

(19) Peterson, I. R.; Brezesinski, V.; Kenn, R. M.; Seitz, R. *Langmuir* **1992**, *8*, 2995.

(20) Overbeck, G. A.; Möbius, D. *J. Phys. Chem.* **1993**, *97*, 7999.

(21) For discussion and references, see: Sirota, E. B. *Langmuir* **1997**, *13*, 3849.

(22) Peterson, I. R. *Ber. Bunsen-Ges. Phys. Chem.* **1991**, *95*, 1417.

(23) Marshall, G.; Teer, E.; Knobler, C. M.; Schalke, M.; Lösche, M. *Colloids Surf. A* **2000**, *171*, 41.